Extending the Velocity Resolution of Waveform Inversion Below the Diving Waves Using AWI

M. Warner[1]*, T. Nangoo[1], A. Pavlov[1], C. Hidalgo[2]

[1] S-Cube; [2] INEOS

Summary

The combination of conventional FWI and adaptive waveform inversion is used to invert a broad-band narrow azimuth shallow-water towed-streamer dataset, recovering an accurate velocity model, to 20 Hz, above, within and below high velocity chalk to a total depth of around 5000 m. FWI alone cannot achieve this depth of penetration from this dataset.

Extending waveform inversion below the diving waves using AWI

Summary

Conventional full-waveform inversion of surface seismic data is normally able to recover an accurate and well-resolved velocity model down to the depth of penetration of the deepest recorded diving waves. This depth depends upon the acquisition geometry and the background velocity model, but it seldom extends much deeper than about 2 to 3 km below mud line, and can be shallower where there are strong velocity inversions. Below this depth, conventional FWI applied directly to reflection data can usefully update the high-wavenumber velocity model but normally makes little useful contribution to longer wavelengths. Various flavours of reflection FWI, that attempt to separate the migration and tomographic aspects of FWI, are capable of modifying the long-wavelength velocity model successfully below the diving waves, but typically such updates have rather poor vertical resolution and are often only able to make relatively minor adjustments to an already-mature velocity model.

Here, we apply adaptive waveform inversion (AWI) (Warner & Guasch, 2016) to a conventional NATS dataset from the Danish sector of the North Sea, recovering the velocity model to 5-km depth including a highly anisotropic low-velocity clastic section underlying thick high-velocity chalk. We used an inversion scheme that interleaves AWI and FWI, and that takes advantage of AWI's enhanced sensitivity to reflection moveout, and lack of edge effects below high-velocity refractors, to build a model which is well resolved over a kilometre below the diving wave zone with the model verified by downhole sonics.

Introduction

AWI was originally introduced as a means of overcoming cycle skipping during waveform inversion. However AWI has two useful additional properties that can enable it to recover long and intermediate-wavelength velocity models below diving waves when conventional FWI fails to do so. AWI has enhanced sensitivity to differences in reflection moveout. This is because the temporal lags of reflection-generated coefficients in the AWI matching-filters relate directly to moveout differences between predicted and observed datasets, whereas the equivalent misfit measured by conventional FWI relates only indirectly to moveout differences through their effect on instantaneous differences in amplitude. Consequently, AWI tends to separate the effects of phase and amplitude differences for reflections helping to differentiate migration and tomographic model updates. In contrast, FWI tends to confuse the two effects, partly mapping a required tomographic velocity update unhelpfully into a change in reflection amplitude, and a mapping a required migration update unhelpfully into a spurious long-wavelength tomographic update designed only to fit reflection amplitudes more closely.

This difference between the two algorithms is not huge, but in practice, in limited-offset NATS data, it is often sufficient to allow AWI to recover long and intermediate-wavelength velocity updates usefully about a kilometre deeper than is possible for FWI. A contributory factor is also AWI's relative lack of long-wavelength artefacts related to the finite aperture of towed-streamer data which otherwise tends to produce a low-velocity edge effect immediately below the deepest-recorded diving waves in FWI inversions. The resultant combination produces less artefact and more signal in reflection-driven AWI than in its FWI counterpart. However, when the current model is already accurate, it is typically FWI rather AWI that converges more quickly and that is capable of the highest resolution and of accurately phase-locking to the observed data. Consequently, an approach that begins with AWI, switches to FWI as the model improves, then switches back to AWI followed by FWI as the frequency content is gradually increased, can take advantage of the benefits of both methods combined. We apply that approach here.

Dataset & Methodology

We applied combined AWI and FWI to 700 square kilometres of 3D narrow-azimuth towed-streamer data from the shallow-water Danish section of the North Sea. The ten cables per sail line were 8100-

m long, the tow depth was 20 m, and the data were recorded on PGS's broadband GeoStreamer. We inverted only the raw hydrophone data, and included all refractions, reflections, multiples and ghosts directly into the inversion. Other than a low-pass filter at 20 Hz, and retention of only every third source position, the input raw data were unprocessed.

The target lies beneath a thick high-velocity chalk section. An anisotropic starting model came from a conventionally processed legacy dataset. Anisotropy in the shale-dominated clastic section below the chalk is high with epsilon values of up to 40%, and delta values up to 20%, observed regularly. For the waveform inversion, we ran ten iteration blocks, with ten iterations per block. Each iteration used 20% of the total retained shots, that is a fifteenth of the original acquired sources. All ten iterations within the same iteration block were run using the same low-pass filter, and the pass-band of the filter was progressively increased after each ten iterations, beginning from the lowest usable frequencies at about 4 Hz, and ending at about 20 Hz. The frequencies quoted are the dominant frequency in the pass-band used; the highest frequency usefully present in the inversion was about 24 Hz. For the first fifty iterations, we ran 5 AWI followed by 5 FWI inversions, with a maximum frequency of 6 Hz. The second 50 iterations, from 6 to 20 Hz, used FWI alone. In total, the inversion involved 100 iterations through subsets of the data, equivalent in compute cost to about seven passes through all the original shots.

Results

Figure 1 shows horizontal slices through the 6-Hz and final 20-Hz models at depths of 100 m and 3300 m. By 6 Hz, the long-wavelength velocity model is fully developed, but finer structure continues to build as the inversion proceeds. After 6 Hz, the role of AWI is largely complete, and it is FWI that continues to improve the model. The 6 Hz model is adequate for migration here – though that is not always the case in more structurally complex models. Even here, where the macro-model is fairly smooth, including the velocity effect of shallow channels in the migration is beneficial – these channels are not properly imaged on the 6 Hz result. The 20-Hz model correctly captures shallow channels, ties the wells, and is useful for direct interpretation, identifying drilling hazards, determining overpressure, and correcting AVO/AVA effects.
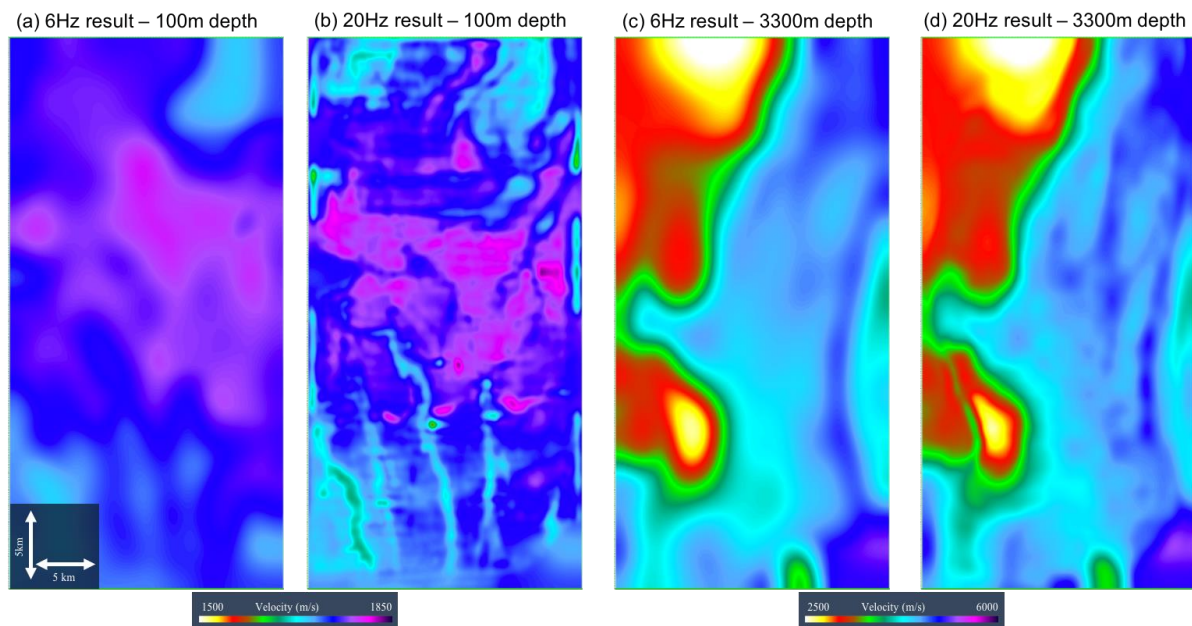

Figure 1 *Depth slices through the recovered velocity model: at 100 m from (a) 6-Hz result, (b) 20-Hz result, and at 3300 m from (c) 6-Hz result, and (d) 20-Hz result.*

Figure 2 shows in-line and cross-line sections through a well location. The well is shown in Figure 3; it was not used to drive or constrain the wavefield inversion, but it and 10 others were used to adjust the anisotropy model in order to tie depths in the wells. Well ties were matched to typically better than 30 m; the well ties were significantly worse when using an earlier anisotropy model inherited from previous tomographic velocity model building. That is, when FWI follows tomography, and the macro model changes as a consequence, it is normally necessary to recalibrate the anisotropy model in order to re-tie the wells.
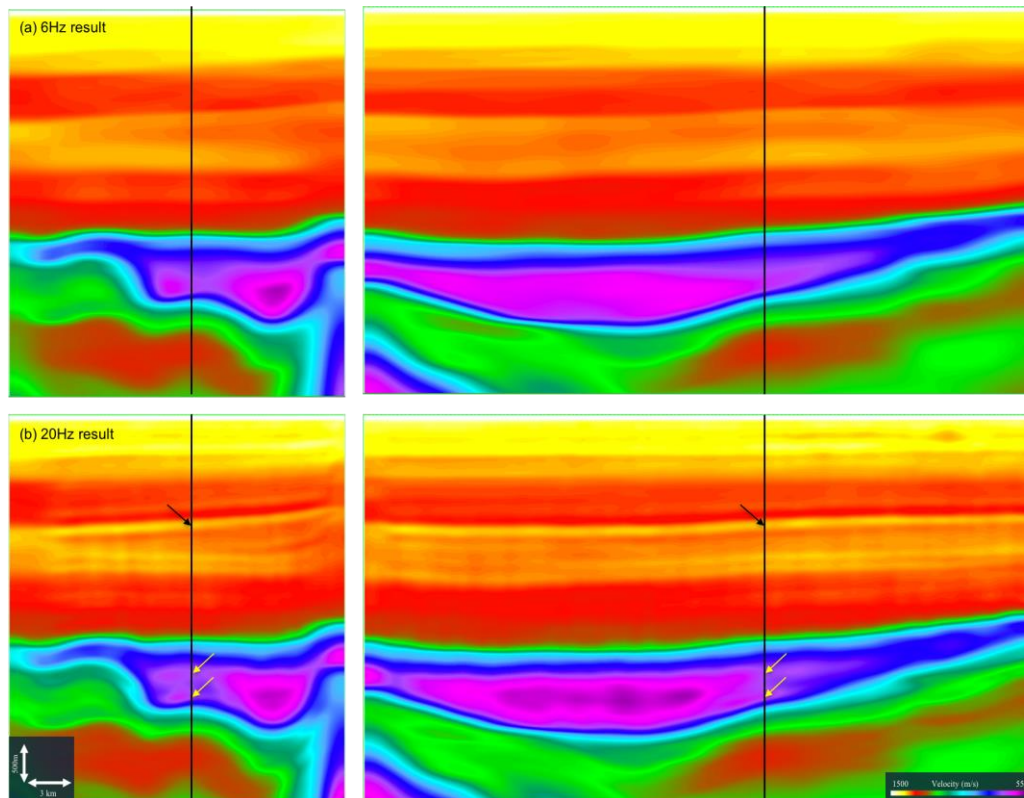

Figure 2   In-line and cross-line vertical depth slices through the recovered velocity model from (a) 6-Hz result, (b) 20-Hz result through the well shown in Figure 3. The arrows show velocity features that are visible in the well. The sections shown extend from the surface to 5000 m depth.

Figure 3 shows a comparison of the recovered velocity model and sonics recorded in the well shown on Figure 2. The recovered model matches the well accurately within the bandwidth of the inversion. The black arrow indicates a sharp kick in velocity that is seen in the well, and that is accurately captured by the waveform inversion model. The yellow arrows indicate the structure in the fast chalk layer where two higher-velocity regions are separated vertically by slightly lower velocities. Again the velocity structure is captured within the bandwidth of the waveform inversion.

Figure 4 shows a comparison of the field data with synthetics for a single shot generated by the low-frequency 6-Hz model, and by the final 20-Hz model. Even the 6-Hz model is able to capture many of fine details of the field data, but the higher-frequency result is required in order to generate the majority of the reflections. The importance of waveform inversion in this study is principally in the improvements introduced within the chalk layer when compared to the legacy velocity model. High velocities in the chalk in the FWI model are now largely conformable with the chalk stratigraphy, and better match the wells; the resulting improvements have served to reduce structural uncertainty at target level below the chalk.
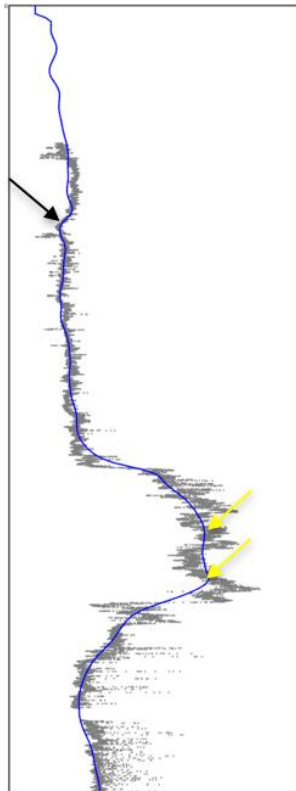
Figure 4 *Modelled shots from (a) the 6-Hz result, (b) the 20-Hz result, and (c) the field data.*

Figure 3 *Comparision of 20-Hz FWI model with sonics in the well shown on Figure 2. The well is 5000 m deep and is shown from the surface. The velocity scale runs from 1000 to 6500 m/s.*
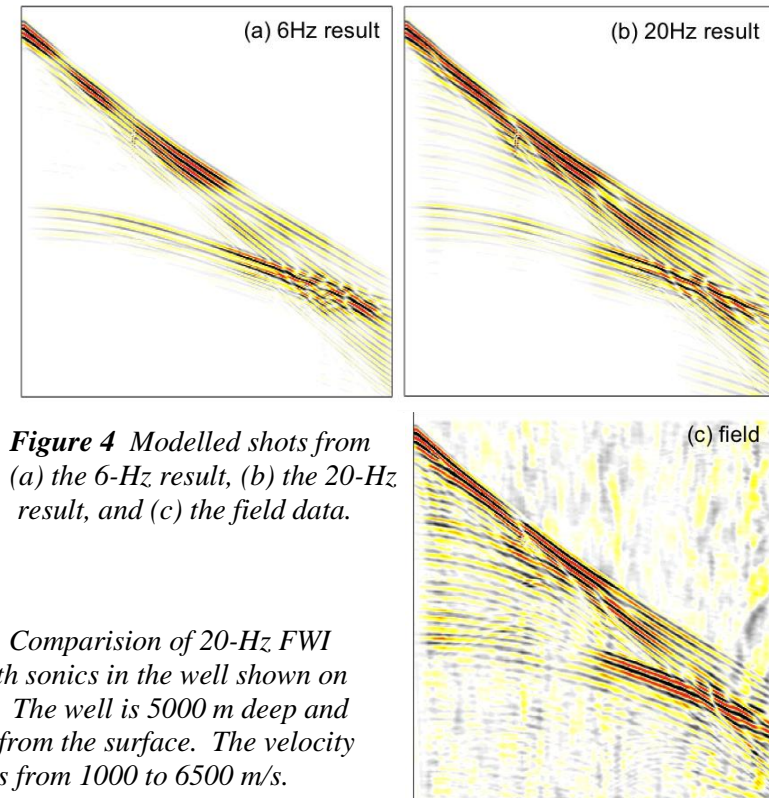
Discussion and Conclusion

The interleaved combination of AWI and conventional FWI has proven powerful in this and a number of other studies. The use of AWI allows inversion to begin from a smoother and less accurate starting model than for FWI alone; this allows for the direct testing and verification of structure in the velocity model that may otherwise simply be inherited from an imperfect starting model. AWI also allows greater penetration in depth than does FWI alone, and it makes more use of reflected arrivals. Including FWI leads to a final model that is well resolved and that is properly phase locked to the field data – something that AWI will struggle to do when used alone. In this study, we have not used pure reflection FWI to build the model to greater depth still, but beginning from combined interleaved AWI and FWI can provide a solid foundation for subsequent high-resolution reflection FWI. In companion paper (Debens et al, 2019) we follow that approach, including the three-way combination of FWI, AWI and RWI.

Acknowledgements

References

Warner, M. & Guasch, L. [2016] Adaptive waveform inversion: Theory. *Geophysics*, **81**, R429-R445.

Debens, H. et al [2019] Penetrating below the diving waves with RWI, AWI and FWI: a NWS Australian case study. 81st EAGE Conference & Exhibition, Extended Abstracts.